Trinucleosome Compaction Studied by Fluorescence Energy Transfer and Scanning Force Microscopy

Malte Bussiek, Katalin Tóth, Nathalie Schwarz, and Jörg Langowski*

Division of Biophysics and Macromolecules, Deutsches Krebsforschungszentrum, Im Neuenheimer Feld 580, TP3, D-69120 Heidelberg, Germany

Received April 25, 2006; Revised Manuscript Received June 30, 2006

ABSTRACT: The effect of the salt concentration, linker histone H1, and histone acetylation on the structure of trinucleosomes reconstituted on a 608 bp DNA containing one centered nucleosome positioning signal was studied. Fluorescence resonance energy transfer (FRET) in solution and scanning force microscopy (SFM) measurements in liquid were done on the same samples. The distance between the DNA ends decreases under the effect of an increasing salt concentration and also by the incorporation of the H1 linker histone. A decrease of internucleosomal center-to-center (cc) distances by H1 was observed that was limited to a minimal value of about 20 nm. The distribution of the angle formed between consecutive nucleosomes was narrowed by H1. The effect of acetylation of all histones leads to decompaction, measured as an increased distance between the DNA ends, and also increased the internucleosomal distances. Selective acetylation of histone H4, however, compacts the structure as measured by FRET.

While the structure of the mono- and tetranucleosome has been determined crystallographically to atomic resolution (*1*−*4*), the arrangement of nucleosomes into a higher order chromatin fiber in solution is still a controversial question. Nucleosomes are arranged in a regular "beads-on-a-string" structure on the DNA and are separated by variable-length segments of free "linker DNA". Typical nucleosome repeats range between 170 and 210 bp (*5*, *6*). The common view is that this chain then condenses into a "30 nm fiber" (*7*, *8*), whose conformation can be modulated by factors such as buffer conditions, associated proteins, and histone modifications. The compaction state of chromatin is known to depend upon the ambient salt concentration, reflecting the electrostatic component of the histone−DNA interaction (*9*, *10*). Linker histones (*11*−*13*) associate to the linker DNA outside the nucleosome core, forming a so-called "nucleosome stem" (*13*). They participate in the stabilization of the condensed state of chromatin and can be associated with the deactivation of DNA-dependent metabolic processes (*14*). The covalent modification of histones plays a central role in the regulation of the active and inactive state of chromatin. In particular, histone acetylation has been associated with actively transcribed chromatin and deacetylation with inactivation or silencing (*15*).

The mechanisms of chromatin activation or deactivation are closely related to the, still debated, morphology of the condensed chromatin fiber. According to the solenoid model, consecutive nucleosomes are closely packed and are helically arranged along the fiber (*7*, *16*). In the "zigzag" model derived from cryo-electron microscopy imaging, linker DNAs are straight (*12*) and nucleosomes form a two-start helix (*4*, *17*). This structure is stabilized by lateral interactions between nucleosomes i and $i + 2$ and a linker histone-induced reduction of the angle between the DNA entering and exiting the nucleosomes (*12*, *13*, *18*−*22*). Recent work, including the crystallographic structure of a cross-linked tetranucleosome, seems to favor a straight-linker zigzag structure (*4*), but the controversy is not fully resolved (*23*).

One approach to study the oligonucleosome structure in solution and determine possible changes in the compaction state is to determine distances between characteristic features within or between nucleosomes, varying external conditions including the buffer composition, the presence of linker histone, or the length of the linker DNA. A reliable method to determine intramolecular distances in biomolecules and their changes is fluorescence resonance energy transfer (FRET),[1] i.e., the transfer of excitation energy from a donor fluorophore to an acceptor. The FRET efficiency depends upon the inverse 6th power of the distance and is a good measure for the donor−acceptor distance in the range of 2−10 nm. It has also been called the "molecular ruler" (*24*).

Using FRET measurements on reconstituted mononucleosomes, we previously showed that the incorporation of linker histone H1 decreases the distance between the linker arms over their whole length (*20*, *22*). This agrees with the earlier observed extended "stem" structure formed between linker DNAs and linker histones outside the nucleosome core (*13*, *19*). Recently, we could show that acetylation of H3 and H4 exhibits differential effects on the local linker DNA geometry (*22*).

Detailed structural information on large biomolecular complexes can be obtained by scanning force microscopy (SFM), which allows for the imaging of surface-bound

* To whom correspondence should be addressed: Division of Biophysics and Macromolecules, Deutsches Krebsforschungszentrum, Im Neuenheimer Feld 580, TP3, D-69120 Heidelberg, Germany. Telephone: 06221/423390. Fax: 06221/423391. E-mail: jl@dkfz.de.

[1] Abbreviations: FRET, fluorescence resonance energy transfer; SFM, scanning force microscopy; cc, center-to-center.

10.1021/bi060807p CCC: $33.50 © 2006 American Chemical Society
Published on Web 08/18/2006

biomolecules with nanometer resolution under near-native conditions (i.e., in buffer). For instance, we showed the formation of bulge defects on nucleosomes reconstituted on superhelical DNA (*25*), and also the effect of H1 binding on mononucleosomal linker DNA geometry was analyzed by SFM (*21*). Numerous other examples exist in the literature, where SFM has been used to characterize the structure of oligonucleosomes and chromatin fibers (*26*−*30*).

Expanding on our mononucleosome work, we characterize here sizes and shapes of trinucleosomes in different compaction states by FRET and SFM. To this goal, we reconstituted trinucleosomes on 608 bp long DNA fragments containing one positioning sequence in the center with recombinant unmodified or differently acetylated histone octamers in saturating stoichiometry and studied the effect of ionic conditions and/or the incorporation of linker histone H1.

FRET was used to measure the average distance between the two fluorescently labeled ends of the trinucleosomal DNA. This distance depends upon different factors: the position and relative orientation of the octamers and the length and mobility of the terminal DNAs. All of these factors may be influenced by the electrostatic conditions and post-translational histone modifications such as acetylation. A variation in the length of the free DNA termini, which depends upon nucleosome positioning, may also influence the end-to-end distance. FRET distances measured in bulk are averages over the whole solution, and because of the $1/R^6$ dependence of the energy transfer, smaller distances strongly dominate this average. Information about the inhomogeneity of the population cannot be obtained from steady-state FRET measurements in bulk solution. For further structural information, the FRET studies were thus complemented by SFM, producing a relief image of the molecules attached to a surface. The images allow us to quantify directly the distances between the centers of successive nucleosomes, the central angle between the three nucleosomes, and the regularity of the positioning. To minimize possible artifacts during the sample preparation and to improve the height resolution, SFM was done on unfixed material in liquid, without drying the samples prior to imaging.

MATERIALS AND METHODS

DNA. A DNA fragment of 608 bp containing the nucleosome positioning sequence of the *Xenopus borealis* 5S rRNA gene in the center was prepared by PCR amplification using two primers equidistant from the +1 position of the corresponding sequence in the plasmid pXP10 (courtesy of Stefan Dimitrov, Grenoble, France). The primers were labeled through a C_6 carbon linker on their 5′ end either with rhodamine X (Thermo Hybaid GmbH, Ulm, Germany) or with Alexa 488 (in our laboratory). Purification and gel controls were done as described (*20*). Sequences of the DNA fragment and the primers are given in the Supporting Information.

Histones. Recombinant core histones of *Xenopus laevis* were expressed in *Escherichia coli* as described (*31*). The histones were acetylated individually by acetyl phosphate as described in ref *22*. Histone octamers were reconstructed from nonacetylated histones, from mixtures where only H3 and/or H4 were acetylated or where all histones were acetylated; acetylation and octamer stoichiometry was controlled by gel electrophoresis (*22*). Histone H1 was purchased from Roche Diagnostics (Mannheim, Germany) and used after purification on Sepharose and NAP-5 columns (Pharmacia).

Trinucleosome Reconstitution. Histone octamers and DNA fragments were mixed in TE buffer at 2 M NaCl in reaction volumes of 50−100 μL. The DNA fragment concentration was 0.4 M, and an octamer/DNA molar proportion of up to 6:1 was used. This high proportion of octamers turned out to be necessary for fully loading the 607 bp DNA with three nucleosomes. The reconstitutions were started at room temperature for 30 min and then were dialyzed against stepwise decreasing NaCl concentrations down to 5 mM in minidialyzing tubes (Pierce, Rockford, IL) at 4 °C. H1 was added at 0.6 or 0.4 M NaCl in a molar proportion of 3:1 over the DNA fragments. The reconstitutions were controlled by electrophoresis in 1% agarose gels run in TBE buffer. The gel quantification was done using the program Intelligent Quantifier version 2.8 (Bioimage, Jackson, MI).

FRET. Fluorescence emission spectra with donor excitation at 495 nm and acceptor excitation at 585 nm were measured with an SLM-AMINCO 8100 fluorescence spectrometer (SLM, Urbana, IL) using a 150 W xenon lamp. FRET efficiency was calculated from the enhanced emission of the acceptor as described (*22*). Aggregation of the sample, producing interparticle FRET, was excluded by the control of the absorption spectra and the Rayleigh peak in the fluorescence. Free DNA was taken into account as calculated from gel quantification.

SFM. SFM was done with a Nanoscope IIIa, software version 5.12 (Digital Instruments, Santa Barbara, CA) and type NP-S20 silicon nitride probes (Veeco Instruments, Plainview, NY). Mica was pretreated by incubation with 30 μL of a 4 μg/mL poly-L-lysine solution for 30 s and subsequent rinsing with water and drying, yielding a surface to which DNA binds irreversibly at a low salt concentration (*32*). The reconstituted chromatin particles were diluted to a concentration of about 5 nM in 10 mM HEPES-NaOH at pH 8.0 and 10 mM NaCl and then adsorbed to the PL mica. Scanning was done directly in the adsorption buffer with a set point of 0.3−0.4 V, a scan size of 1 × 1 or 2 × 2 μm, a scan rate of 1−2 Hz, and a resolution of 512 × 512 pixels. Images were flattened, and trinucleosomes were isolated from the scans by producing 130 × 130 nm zooms for the following measurements. We measured center-to-center (cc) distances between adjacent nucleosomes either as the sum of twice the nucleosome radius and the linker DNA length when it was distinguishable or as the direct distance between the two mass centers if no linker DNA was seen. The internucleosomal angle was defined as the central angle between the three nucleosome centers.

RESULTS AND DISCUSSION

Distance between Trinucleosomal DNA Ends. Trinucleosomes were prepared from fluorescently end-labeled 608 bp long DNA and a saturating amount of histone octamers (six octamers per DNA molecule at our conditions). We used Alexa 488 and rhodamine X as donor and acceptor dyes representing a Förster radius of 5.5 nm at low salt conditions (*20*). It has been shown earlier that FRET may be used with

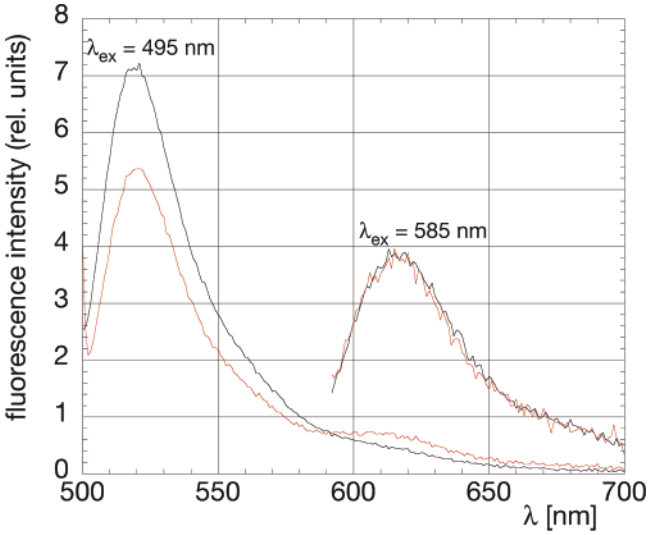

FIGURE 1: Fluorescence emission spectra of two selected trinucleosome samples: low FRET sample (black lines, H3 acetylated, 5 mM NaCl) and high FRET sample (red lines, H4 acetylated, 75 mM NaCl). Donor excitation (at 495 nm) was used for the detection of the FRET signal, and acceptor excitation (at 585 nm) was used for the comparison of the concentrations. Spectra are corrected for the baseline because of the buffer, for the instrument characteristics, and for the concentration.

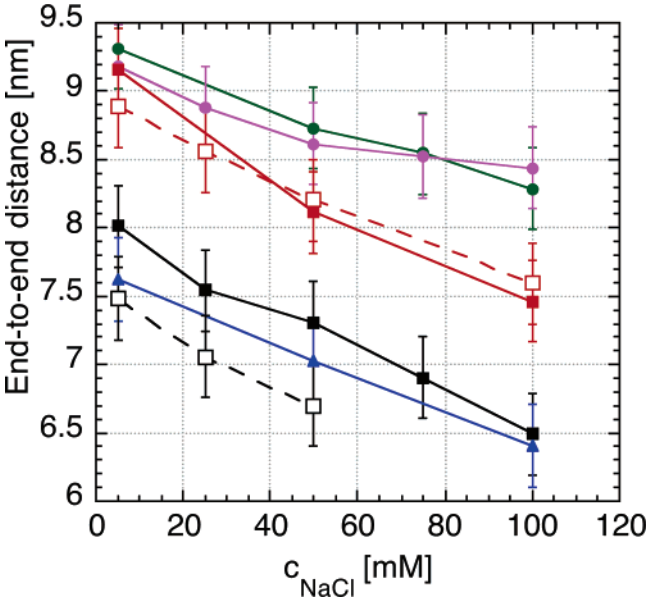

FIGURE 2: Dependence of the trinucleosomal DNA end-to-end distances on the salt concentration, histone acetylation state, and incorporation of linker histone H1 as measured by FRET. Trinucleosomes were reconstituted from unmodified histone octamers (black), from octamers where only H4 (blue) or H3 (green) are acetylated, and where both H3 and H4 (purple) or all histones are acetylated (red). Empty symbols represent the presence of H1.

dye pairs of such Förster radii to measure the distance in the range between 6 and 9 nm, e.g., for determining DNA curvature (*33*). The photophysics of both of these dyes are largely pH-independent. The salt dependence of their fluorescence was measured on donor-only- and acceptor-only-labeled samples. The Förster radius was found to decrease slightly (from 5.5 to 5.2 nm) in the salt concentration range used (*22*), and this was taken into account in the distance calculations. There was no significant change in the anisotropy of either dye under all of our conditions. The FRET spectra changes from free DNA to trinucleosomes and also between the differently acetylated trinucleosomes depending upon the presence of linker histones and the salt concentration. Representative spectra are given in Figure 1. Figure 2 shows the FRET-measured averaged end-to-end distances for the complexes, as a function of the NaCl concentration in the presence or absence of linker histone H1 and for different acetylation states of the core histones. The distances are in all cases smaller than 10 nm, the diameter of a single nucleosome. Using subsaturating octamer/DNA proportions (2:1 or 4:1), producing mainly mono- or dinucleosomes, no measurable FRET was obtained; thus, the corresponding averaged DNA end-to-end distances were larger than 11 nm (data not shown).

The binding of histones to the DNA was controlled in gel retardation experiments. Figure 3 shows images of agarose electrophoresis gels of the trinucleosome samples. Generally, a band shift is observed that increases with the amount of histone added up to a stoichiometry of 6:1 (Figure 3A); higher histone/DNA ratios led to strong aggregation (data not shown). The mono- or dinucleosomes observed at lower stoichiometries (Figure 3A) present discrete bands different from those in saturated samples. Dependent upon the acetylation state of the histones, the shifted band may be narrow or broad (Figure 3B). A sharp band at 600 bp of DNA and a variably broad band of slower complexes can be distinguished in all cases. The proportion of the free DNA as determined by quantitative gel analysis varied between 5−10% along the preparations and was taken into account in all FRET calculations.

Geometry of Unmodified Trinucleosomes. The surprisingly small distances between the DNA ends as measured by FRET led us to use SFM to elucidate possible geometries. To reduce preparatory artifacts, we imaged unfixed samples in liquid. Figure 4 presents SFM scans and zoomed images of trinucleosomes, assembled with either unmodified (Figure 4B), acetylated histones (Figure 4D), or also samples that contained the linker histone H1 (Figure 4C). Scanning was carried out in buffer containing 10 mM NaCl, under which conditions a stable binding of the particles to the surface could be reproducibly observed. The overview images show a rather even distribution of the particles on the surface, confirming that aggregation did not cause the occurrence of the FRET signal. The individual particles shown in b−d of Figure 4 were selected to suggest the variability in the arrangement and relative positioning of the three nucleosomes. Where both DNA ends are distinguishable, they are significantly further away than 10 nm. The lack of visible DNA ends in closely packed trinucleosomes, such as shown in c2 of Figure 4, may be due to their folding inside of the complexes. Such conformations would contribute strongly to the FRET, but the DNA end-to-end distance would not be measurable with SFM.

We suppose that the flattening at the surface may have a non-negligible effect on the form of the objects. For instance, an inhomogeneous charge distribution along the particles may be associated with structural rearrangements in a way that a simple projection-like process cannot be assumed. Under our conditions, poly-L-lysine is supposed to bind the DNA to the surface rather than the histones; thus, the strength of the interaction between the trinucleosome and the surface will depend upon the extent of the accessible DNA that can

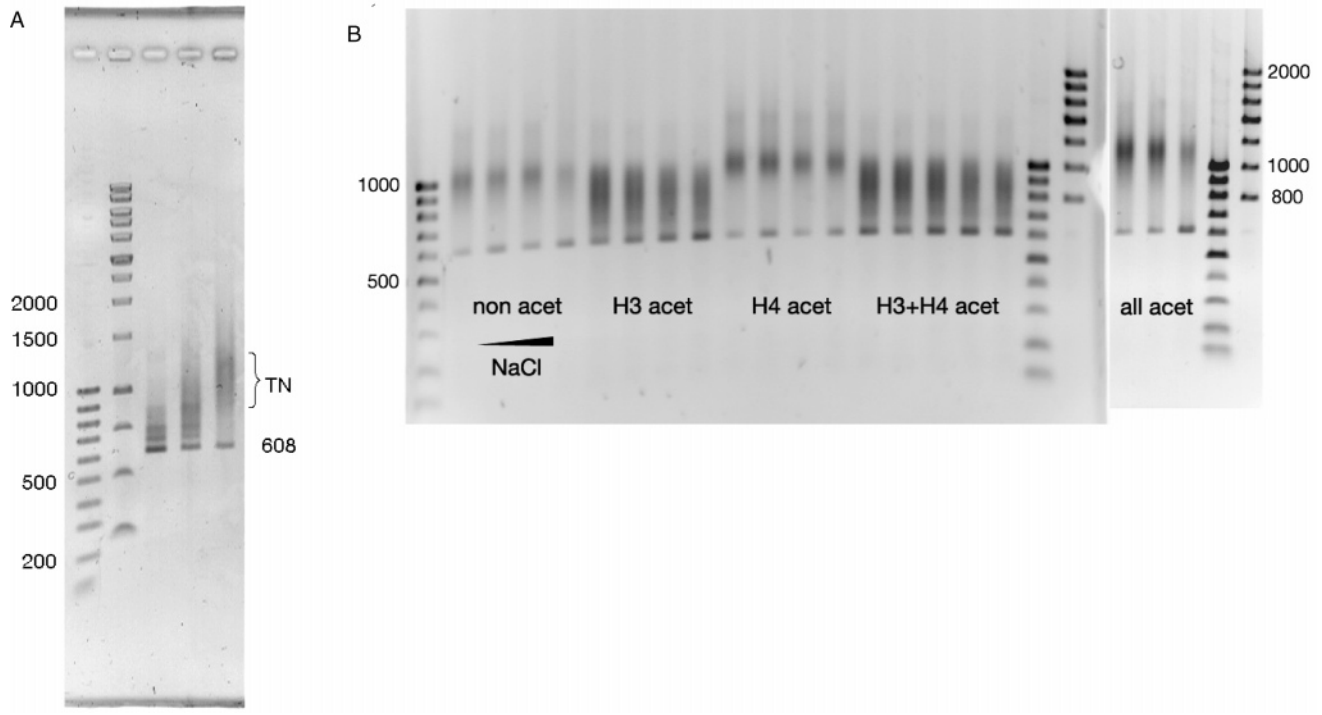

FIGURE 3: Agarose gel electrophoretic analysis of trinucleosomes reconstituted with recombinant histones and 608 bp DNA. (A) Reconstitution of nucleosomes with unmodified histones at different molar ratios of histones/DNA. DNA marker (100 bp, lanes 1) and marker (200 bp, lane 2). Histone octamer/DNA stoichiometry of 2:1 (lane 3), 4:1 (lane 4), and 5.6:1 (lane 5). (B) Reconstitutions with differently acetylated histones and subsequent adjustment to different NaCl concentrations (from 5 to 100 mM). DNA markers (100 bp, lanes 1, 19, and 26) and markers (200 bp, Thermo Hybaid, lanes 22 and 27). Reconstitutions from unmodified histone octamers (lanes 2−5), octamers where only H3 (lanes 6−9), only H4 (lanes 10−13), only H3 and H4 (lanes 14−18) were acetylated, and where all histones were acetylated (lanes 21−23). Marked next to the gel: TN, trinucleosome numbers; DNA lengths in base pairs.

interact. Accordingly, a direct comparison of end-to-end distances measured by FRET and SFM is not justified, but we may get an insight into possible shapes of the complexes and into the homogeneity of the samples.

A parameter that is probably less sensitive to the adhesion process than the DNA end-to-end distance is the distance between consecutive nucleosomes, which rather depends upon the DNA−histone interaction and positioning. Many trinucleosomes appeared closely packed, with no or only small pieces of linker DNA detectable. cc internucleosomal distances were measured on complexes where all three nucleosomes are present and distinguishable, either along the linker DNA contour if it was visible or along a straight connecting line otherwise. Nucleosomes could still be resolved when they were likely to contact each other. Mean nucleosomal heights of 3.6, 4.5, and 4.6 nm (0.8 nm) were obtained with three different silicon nitride probes, in good agreement with the height distribution reported for isolated chicken erythrocyte chromatin (4.2 ± 1.1 nm) (*34*) and our own work on nucleosomes formed on superhelical DNA (*25*). The histograms on Figure 5 show relatively large cc distance distributions and contain one major peak. The presence of this major peak indicates a nonrandom positioning of the outer nucleosomes on the DNA, even though it contains only one central positioning sequence, which is explained by a preference for a localization of nucleosomes in a close neighborhood because of internucleosomal interactions (*35*). For nonacetylated trinucleosomes, the major peak is centered at around 20 nm and the mean value is 27.6 ± 13.2 nm. This value is comparable to those obtained on H1-stripped chromatin fibers isolated from HeLa cells (*36*) or from chicken erythrocytes (*37*). Together with the height values mentioned above, this correspondence suggests that the reconstituted trinucleosomes feature important properties of isolated chromatin fibers.

Salt-Induced Compaction. Increasing the NaCl concentration from 5 to 100 mM enhances the energy transfer by causing the DNA ends to approach by approximately the same amount (1−2 nm) at all acetylation states, independent of the presence of linker histones (Figure 2). This effect is more pronounced than the 0.5−1 nm/100 mM NaCl recently observed on the DNA ends of mononucleosomes with 150−220 bp DNA fragments (*22*). For mononucleosomes, the salt-induced closing of the DNA arms might be explained by simple shielding of the electrostatic repulsion of the linker DNAs; for trinucleosomes, interactions between the core particles may also play a role in the compaction. In Figure 3B, some salt-dependent release of the DNA with an increasing NaCl concentration is apparent. As mentioned earlier, this effect could be accounted for by quantifying the amount of free DNA. The reason for this dissociation may be the very low concentration (100 nM) of the complexes (*38*). At any rate, the release is much less pronounced (10% at 100 mM NaCl) than the 20% observed earlier for mononucleosomes (*22*). A cooperative stabilizing effect of the neighboring nucleosomes may explain the higher stability of the trinucleosomes. The width or structure of the shifted gel bands corresponding to the DNA−histone complexes is not changing significantly with the salt concentration, indicating that any disintegration is an all-or-none process and not a disruption of only one or two nucleosomes. The cations probably also play a more complex role, because they

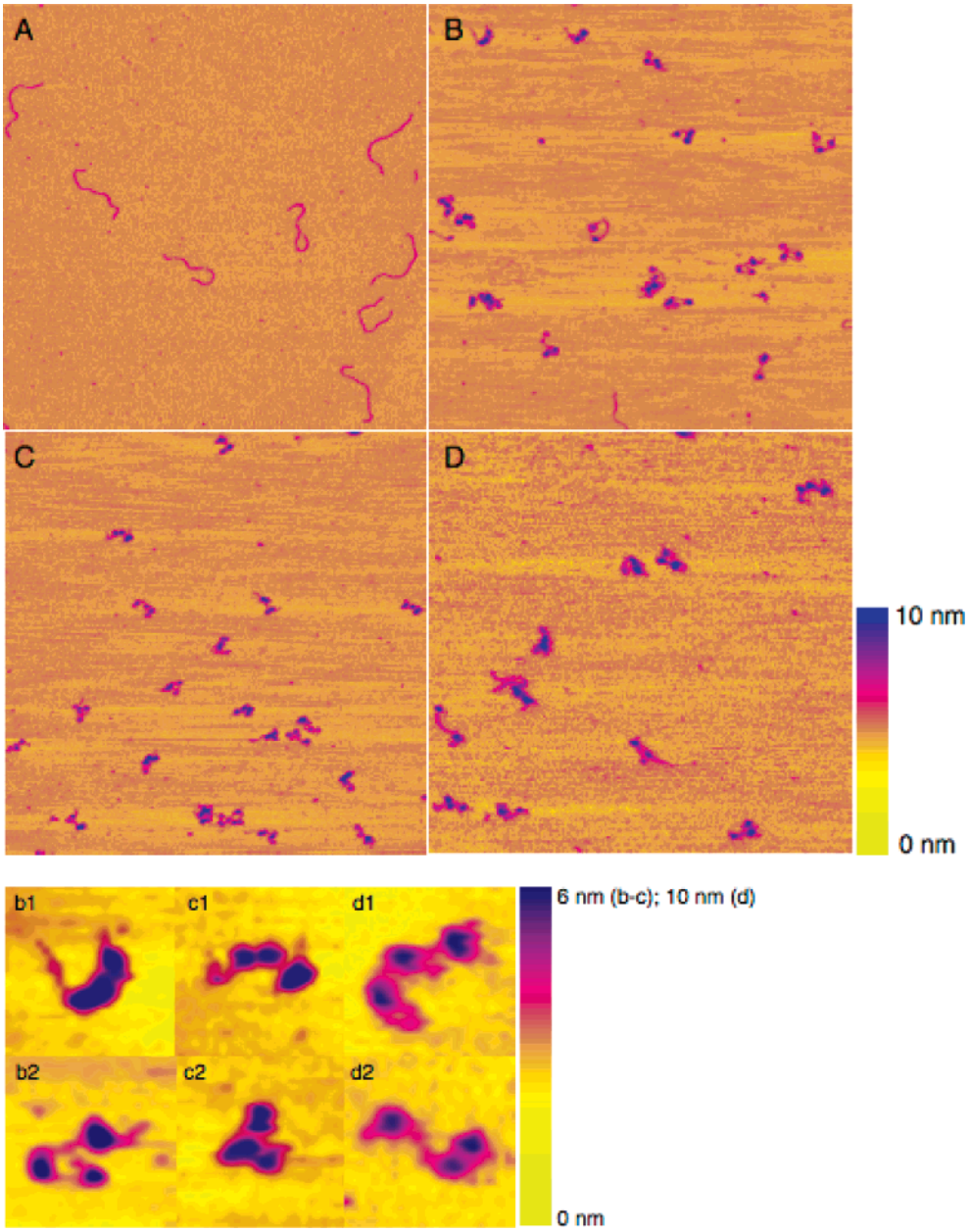

FIGURE 4: SFM images recorded in liquid of free 608 bp DNA (A) and 608 bp DNA reconstituted with unmodified octamers in the absence (B), in the presence of linker histone H1 (C), and with acetylated octamers without linker histone (D). Selected zooms of individual trinucleosomes from unmodified histones in the absence (b1 and b2), in the presence of linker histone H1 (c1 and c2), and from acetylated histone octamers (d1 and d2). The more diffuse appearance of the particles in D (zoom, d) is due to the variation in the scanning tips.

decrease DNA−DNA repulsions and the histone−tail transmitted interactions also change.

At the higher NaCl concentration, the samples were not measurable with SFM in solution, probably because of insufficient adhesion to the surface. This might reflect the more compacted form of the particles, causing less DNA to be exposed to the surface. Changing the poly-L-lysine concentration did not improve the adhesion, and we could not find appropriate conditions in the literature either. Compact trinucleosome conformations could be observed in the presence of $MgCl_2$ after adsorption onto bare mica and imaging after drying the sample, but this procedure also lead to a considerable disruption of nucleosomes. Therefore, the reliability of this preparation method for structural analysis of nucleosome arrays is questionable. Several SFM studies exist about the effects of salt on fixed, air-dried chromatin preparations, and differences between extended low-salt and compact/aggregated high-salt forms were reported, e.g., ref *37*. From measurements of hydrodynamic or solution-scattering parameters, one can also obtain geometrical data, in comparison with models [e.g., the HYDRO program (*39*)]. A salt-dependent increase of the sedimentation coefficient was observed on isolated and reconstituted di- and trinucleosomes in the absence of H1 histones (*10*, *40*). Using the ultracentrifugation data and neutron scattering combined with model calculations, a decrease from 22 to 15 nm could be estimated for the cc distances of H1 containing dinucleosomes between 5 and 100 mM NaCl (*10*).

The salt-dependent compaction of chromatin is a well-known phenomenon that can be compared with theoretical predictions and can serve to estimate the contribution of electrostatic interactions to the chromatin structure. Under

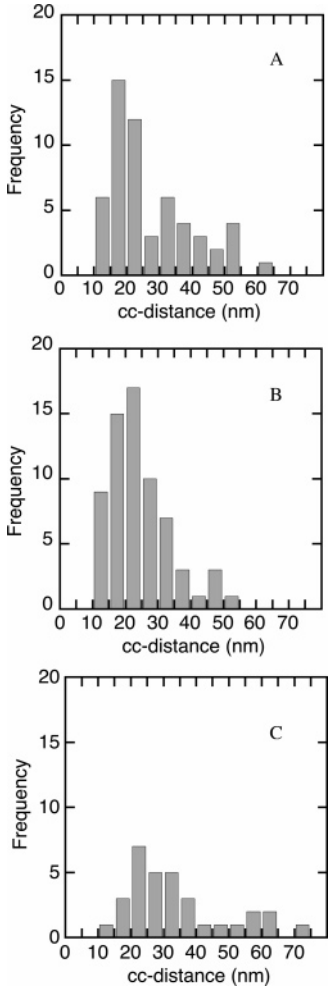

FIGURE 5: Distribution of the SFM-measured cc distances on trinucleosomes from unmodified histone octamers in the absence (A), in the presence (B) of linker histone H1, and from acetylated histone octamers (C).

physiological conditions, however, the buffer environment does not change significantly. Electrostatic effects are nevertheless important because the charge of the histones depends upon the degree of histone acetylation, a central parameter that determines gene activity. In the following, we demonstrate the effect of histone acetylation on the trinucleosome structure.

Effect of Core Histone Acetylation. Recently, we used selective chemical acetylation of the histones to study the linker DNA geometry on mononucleosomes (*22*): acetylation of only H4 causes an approach of the linker DNA ends, while H3 acetylation increases their distance. The effect of combined acetylation of H3 and H4 or of all histones also leads to the opening of mononucleosomal linker arms. The chemical acetylation does not impede the formation of trinucleosomes (see the gel on Figure 3B). The differential effect of chemical acetylation on the trinucleosomal end-to-end distances is very similar to the mononucleosomes and also additive to the salt effects (Figure 2). The smallest averaged end-to-end distance corresponds presumably to the highest compaction level, which is attained with H4-only-acetylated octamers at an increased salt concentration. The homogeneity of the trinucleosome preparations varies according to the acetylation state, as evidenced by the change in width of the gel bands in Figure 3B. For the nonacetylated, H4-only-acetylated, or all-histone-acetylated samples, the band representing the complex is narrow, indicating a rather homogeneous trinucleosome preparation. In the case of H3-only or H3/H4 acetylation, the bands are broad. This may represent a mixture of subsaturated complexes and/or differences in the length or mobility of the DNA ends of trinucleosomes because of inhomogeneous positioning. We also note that there are significant differences in average gel mobility between the samples: both the H3- and H3/H4-acetylated samples migrate faster than the nonacetylated one. This mobility difference could be explained simply by the more negative charge of the acetylated nucleosomes; however, the H4-only-acetylated samples clearly migrate even slower than the nonacetylated ones. Thus, other structural changes must occur upon acetylation that influence the gel migration.

The differential effects of histone acetylation seen in FRET are paralleled by biochemical evidence in several different systems. Mutation of acetylable lysines in the histone tails or complete deletion of those tails showed opposite effects on yeast Gal1 activity for H3 and H4, i.e., an activity increase when H3 tails were deleted or mutated and a strong decrease in the case of H4 (*41*, *42*). More recently, a correlation between H3 acetylation and gene activity but an anticorrelation for H4 was shown for several genes in yeast, including Gal4 (*43*). These in vivo observations suggest that it is not the acetylation per se but the increased (or decreased) compaction that regulates gene activity, in agreement with our FRET observations. However, in contrast to our observations, analytical ultracentrifugation showed a correlation between the acetylation of the single lysine 16 of H4 and the decreased compaction of nucleosome dodecamers in high salt (*44*). How this latter observation on a single lysine acetylation is connected to the effect of the acetylation of multiple lysines (chemically or in vivo) will require further study.

We examined by SFM the geometry of trinucleosomes formed with all histones acetylated (Figure 4D and d1 and d2). Here, we found a higher proportion of incomplete constructs, in agreement with earlier observations on the anticooperative effect of acetylation on the occupation of nucleosome arrays (*45*). The sample shows a larger cc distance distribution with a higher mean value (31.5 ± 10 nm) than that of nonacetylated ones (Figure 5), and the major peak is shifted to 27 nm instead of 20 nm. The relative increase of the mean cc distances by acetylation is the same as in the FRET end-to-end distances (Table 1), indicating that the arrangement of the three nucleosomes determines the terminal DNA geometries as well. A similar trend was observed on fixed longer nucleosome arrays reconstituted from isolated hyperacetylated octamers imaged by SFM (*35*), and it also corresponds to the decompaction postulated from hydrodynamic and electron microscopic observations on hyperacetylated isolated chromatin fibers (*46*). Further SFM studies on trinucleosomes from selectively acetylated histones and a comparison with naturally hyperacetylated trinucleosomes are under way.

Compaction by Linker Histone H1. The incorporation of linker histone H1 reduces the distance between the DNA ends of trinucleosomes formed from nonacetylated histones by about 0.5 nm according to the FRET measurements, while the same amount of added H1 does not cause a significant

Table 1: DNA End-to-End and Internucleosomal cc Distances Determined in this Study by FRET or SFM Measurements on Trinucleosomes

	FRET end-to-end average		SFM cc		
			peak	average	
	nm	relative	nm	nm	relative
core histones unmodified7.9 ± 0.3	7.4 ± 0.3	1	20	27.6 ± 13.2	1
core histones unmodified plus H1	9 ± 0.3	0.94	20	24.3 ± 9	0.88
all core histones acetylated		1.14	27	31.5 ± 10	1.14

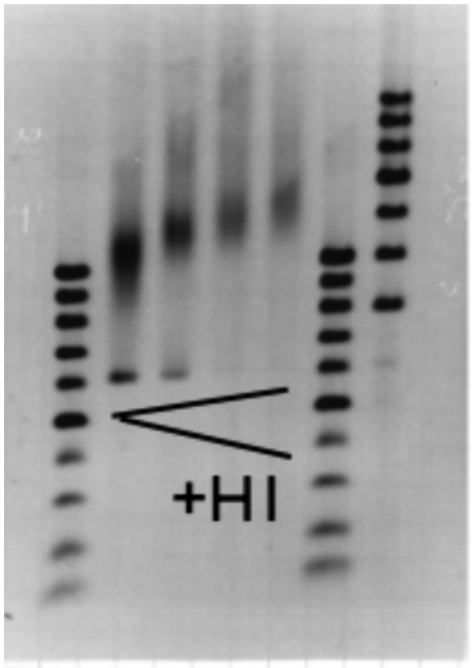

FIGURE 6: Agarose gel electrophoretical characterization of the reconstitutions from unmodified histone octamers with increasing amounts of linker histone H1. DNA markers (100 bp, lanes 1 and 6) and markers (200 bp, lane 7). H1/DNA stoichiometry of 0:1 (lane 2), 1:1 (lane 3), 2:1 (lane 4), and 3:1 (lane 5).

change when all histones are acetylated. The compacting effect of H1 on nonacetylated chromatin and oligonucleosomes is already known from microscopic and hydrodynamic studies (*11*). We observed earlier by FRET measurements on nonacetylated mononucleosomes that the linker DNAs approach each other significantly over their whole length when H1 is incorporated. For unmodified recombinant histones, this change is about 1−1.5 nm (*22*) and slightly less (0.8−1 nm) when one or all histones are acetylated (Tóth, unpublished).

The incorporation of the linker histone into the trinucleosomes is demonstrated by increased gel retardation (Figure 6). We also tried to look for the position of the interaction of the linker histone by MNase digestion. This assay works very well for mononucleosomes. We observed that the MNase digestion of the trinucleosomes is about 3 times slower in the presence of H1, but the expected band at around 170 bp could not be detected in any of the samples (not shown).

Linker Histone H1 Regularizes the Structure. The trinucleosomes containing linker histone H1 appear more compact on the SFM images (Figure 4C and c1 and c2). Also, in agreement with the gel pattern, less free DNA appears in the image. The incorporation of the H1 slightly reduces the mean cc distance (24.3 ± 9 nm); however, the most frequent cc distance at 20 nm is not changed (Figure 5). This 20 nm

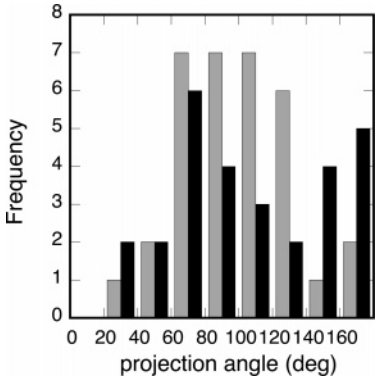

FIGURE 7: Distribution of the SFM-measured projection angles for trinucleosomes from unmodified histones in the absence (black) and presence (gray) of linker histone H1.

distance may represent the minimum to which H1 can "pull together" neighboring nucleosomes, compatible with the earlier described "stem" structure formed between the linker histone and linker DNAs (*13*, *47*). The proportion of higher cc distances decreases strongly, suggesting that H1 stabilizes the DNA wrapping around the core histones and/or the positioning. Also, in the presence of H1, there are twice as many (40%) of the complexes where the DNA ends are not resolved by SFM. The characteristic distances obtained from FRET and SFM measurements are collected in Table 1.

The linker histones reduce the entry−exit angle between linker arms, as seen by cryo-electron microscopy of nucleosome arrays (*13*), and they decrease the internucleosomal angle as measured on fixed dried samples by SFM (*48*). Here, we measured the distribution of internucleosomal angles defined by the three centers. The corresponding histograms (Figure 7) show that H1 causes this distribution to change. A broad bimodal distribution in the absence of H1 is narrowed in the presence of H1, while the mean values of 60−80° do not change significantly.

The H1-induced changes in the internucleosomal distance and angle in liquid are in quantitative agreement with earlier findings from SFM (*37*, *48*−*51*), analytical ultracentrifugation and cryo-electron microscopy (*11*), and neutron scattering (*52*).

CONCLUSION

SFM and FRET yield complementary information on the trinucleosome structure. FRET measures the distances between the fluorescently labeled ends of the DNA fragment; these distances are below 10 nm, significantly smaller than even the cc distance of the nucleosomes as measured by SFM. This difference can be explained with the $1/R^6$ dependence of the FRET efficiency, which leads to a much stronger weighting of small distances. Structures where the DNA ends are hidden inside, which are present to a

significant extent in the SFM images, will therefore constitute the main part of the measured FRET.

Trinucleosomes are the smallest unit of chromatin that can mimic the steric conditions and interactions in the zigzag chromatin fiber structure. Here, we have used a 608 bp DNA fragment with one central-positioning sequence, on which nucleosomes were reconstituted by salt dialysis, to gather structural information. As shown by gel electrophoresis and SFM, we obtain very good reconstitution into trinucleosomes with only little free DNA or DNA carrying less than three nucleosomes. FRET measurements demonstrate the compaction of the structure by linker histone H1: the presence of the linker histone H1 leads to a decrease in the FRET-measured end-to-end distance of about 0.5 nm on the nonacetylated trinucleosomes, independent of the salt concentration. Chemical acetylation either of all histones, of H3 only, or of H3/H4 results in a significant opening of the structure, while acetylation of H4 only closes the structure slightly, in agreement with our earlier measurement on mononucleosomes. In the all-acetylated sample, H1 does not seem to affect the end-to-end distance. The SFM images show a narrowing of the distribution of internucleosome distances by H1 but without a significant change in the mean distance. Acetylation, however, leads to an opening of the trinucleosome structure manifested by a significant increase in the mean internucleosome distance.

In summary, we could show here that the same parameters that determine changes of the mononucleosomal linker arm conformation (*22*) also affect the compaction state of the trinucleosomes. This strongly suggests a determining role of the linker DNA geometry for the conformation of the chromatin fiber and its biological function.

ACKNOWLEDGMENT

We thank Maria Mildenberger for technical assistance and Stefan Dimitrov for providing the template for the 608 bp DNA fragment.

SUPPORTING INFORMATION AVAILABLE

Sequence of the 608 bp DNA used for trinucleosome reconstitution (Figure S1). This material is available free of charge via the Internet at http://pubs.acs.org.

REFERENCES

1. Luger, K., Mäder, A. W., Richmond, R. K., Sargent, D. F., and Richmond, T. J. (1997) Crystal structure of the nucleosome core particle at 2.8 Å resolution, *Nature 389*, 251−260.
2. Richmond, T. J., and Davey, C. A. (2003) The structure of DNA in the nucleosome core, *Nature 423*, 145−150.
3. Davey, C. A., Sargent, D. F., Luger, K., Maeder, A. W., and Richmond, T. J. (2002) Solvent mediated interactions in the structure of the nucleosome core particle at 1.9 Å resolution, *J. Mol. Biol. 319*, 1097−1113.
4. Schalch, T., Duda, S., Sargent, D. F., and Richmond, T. J. (2005) X-ray structure of a tetranucleosome and its implications for the chromatin fibre, *Nature 436*, 138−141.
5. van Holde, K. E. (1989) *Chromatin*, Springer, Heidelberg, Germany.
6. Widom, J. (1992) A relationship between the helical twist of DNA and the ordered positioning of nucleosomes in all eukaryotic cells, *Proc. Natl. Acad. Sci. U.S.A. 89*, 1095−1099.
7. Finch, J. T., and Klug, A. (1976) Solenoidal model for superstructure in chromatin, *Proc. Natl. Acad. Sci. U.S.A. 73*, 1897−1901.
8. Adkins, N. L., Watts, M., and Georgel, P. T. (2004) To the 30-nm chromatin fiber and beyond, *Biochim. Biophys. Acta 1677*, 12−23.
9. Gerchman, S. E., and Ramakrishnan, V. (1987) Chromatin higher-order structure studied by neutron scattering and scanning transmission electron microscopy, *Proc. Natl. Acad. Sci. U.S.A. 84*, 7802−7806.
10. Hammermann, M., Tóth, K., Rodemer, C., Waldeck, W., May, R. P., and Langowski, J. (2000) Salt-dependent compaction of di- and trinucleosomes studied by small-angle neutron scattering, *Biophys. J. 79*, 584−594.
11. Carruthers, L. M., Bednar, J., Woodcock, C. L., and Hansen, J. C. (1998) Linker histones stabilize the intrinsic salt-dependent folding of nucleosomal arrays: Mechanistic ramifications for higher-order chromatin folding, *Biochemistry 37*, 14776−14787.
12. Bednar, J., Horowitz, R. A., Dubochet, J., and Woodcock, C. L. (1995) Chromatin conformation and salt-induced compaction: Three-dimensional structural information from cryoelectron microscopy, *J. Cell Biol. 131*, 1365−1376.
13. Bednar, J., Horowitz, R. A., Grigoryev, S. A., Carruthers, L. M., Hansen, J. C., Koster, A. J., and Woodcock, C. L. (1998) Nucleosomes, linker DNA, and linker histone form a unique structural motif that directs the higher-order folding and compaction of chromatin, *Proc. Natl. Acad. Sci. U.S.A. 95*, 14173−14178.
14. Ding, H. F., Bustin, M., and Hansen, U. (1997) Alleviation of histone H1-mediated transcriptional repression and chromatin compaction by the acidic activation region in chromosomal protein HMG-14, *Mol. Cell. Biol. 17*, 5843−5855.
15. Brown, C. E., Lechner, T., Howe, L., and Workman, J. L. (2000) The many HATs of transcription coactivators, *Trends Biochem. Sci. 25*, 15−19.
16. Thoma, F., Koller, T., and Klug, A. (1979) Involvement of histone H1 in the organization of the nucleosome and of the salt-dependent superstructures of chromatin, *J. Cell Biol. 83*, 403−427.
17. Dorigo, B., Schalch, T., Kulangara, A., Duda, S., Schroeder, R. R., and Richmond, T. J. (2004) Nucleosome arrays reveal the two-start organization of the chromatin fiber, *Science 306*, 1571−1573.
18. Furrer, P., Bednar, J., Dubochet, J., Hamiche, A., and Prunell, A. (1995) DNA at the entry−exit of the nucleosome observed by cryoelectron microscopy, *J. Struct. Biol. 114*, 177−183.
19. Hamiche, A., Schultz, P., Ramakrishnan, V., Oudet, P., and Prunell, A. (1996) Linker histone-dependent DNA structure in linear mononucleosomes, *J. Mol. Biol. 257*, 30−42.
20. Tóth, K., Brun, N., and Langowski, J. (2001) Trajectory of nucleosomal linker DNA studied by fluorescence resonance energy transfer, *Biochemistry 40*, 6921−6928.
21. Kepert, J. F., Fejes Tóth, K., Caudron, M., Mucke, N., Langowski, J., and Rippe, K. (2003) Conformation of reconstituted mononucleosomes and effect of linker histone H1 binding studied by scanning force microscopy, *Biophys. J. 85*, 4012−4022.
22. Tóth, K., Brun, N., and Langowski, J. (2006) Chromatin compaction at the mononucleosome level, *Biochemistry 45*, 1591−1598.
23. Huynh, V. A., Robinson, P. J., and Rhodes, D. (2005) A method for the in vitro reconstitution of a defined "30 nm" chromatin fibre containing stoichiometric amounts of the linker histone, *J. Mol. Biol. 345*, 957−968.
24. Clegg, R. M. (1992) Fluorescence resonance energy transfer and nucleic acids, *Methods Enzymol. 211*, 353−388.
25. Bussiek, M., Tóth, K., Brun, N., and Langowski, J. (2005) DNA-loop formation on nucleosomes shown by in situ scanning force microscopy of supercoiled DNA, *J. Mol. Biol. 345*, 695−706.
26. Zlatanova, J., and Leuba, S. H. (2003) Chromatin fibers, one-at-a-time. *J. Mol. Biol. 331*, 1−19.
27. Leuba, S. H., and Bustamante, C. (1999) Analysis of chromatin by scanning force microscopy, *Methods Mol. Biol. 119*, 143−160.
28. Bustamante, C., Zuccheri, G., Leuba, S. H., Yang, G. L., and Samori, B. (1997) Visualization and analysis of chromatin by scanning force microscopy, *Methods Enzymol. 12*, 73−83.
29. Fritzsche, W., Schaper, A., and Jovin, T. M. (1995) Scanning force microscopy of chromatin fibers in air and in liquid, *Scanning 17*, 148−155.
30. Leuba, S. H., Yang, G., Robert, C., Samori, B., van Holde, K., Zlatanova, J., and Bustamante, C. (1994) Three-dimensional structure of extended chromatin fibers as revealed by tapping-mode scanning force microscopy, *Proc. Natl. Acad. Sci. U.S.A. 91*, 11621−11625.
31. Luger, K., Rechsteiner, T. J., and Richmond, T. J. (1999) Expression and purification of recombinant histones and nucleosome reconstitution, *Methods Mol. Biol. 119*, 1−16.

32. Bussiek, M., Mucke, N., and Langowski, J. (2003) Polylysine-coated mica can be used to observe systematic changes in the supercoiled DNA conformation by scanning force microscopy in solution, *Nucleic Acids Res. 31*, e137.
33. Tóth, K., Sauermann, V., and Langowski, J. (1998) DNA curvature in solution measured by fluorescence resonance energy transfer, *Biochemistry 37*, 8173−8179.
34. Fritzsche, W., and Henderson, E. (1996) Scanning force microscopy reveals ellipsoid shape of chicken erythrocyte nucleosomes, *Biophys. J. 71*, 2222−2226.
35. Yodh, J. G., Woodbury, N., Shlyakhtenko, L. S., Lyubchenko, Y. L., and Lohr, D. (2002) Mapping nucleosome locations on the 208-12 by AFM provides clear evidence for cooperativity in array occupation, *Biochemistry 41*, 3565−3574.
36. Kepert, J. F., Mazurkiewicz, J., Heuvelman, G. L., Fejes Tóth, K., and Rippe, K. (2005) NAP1 modulates binding of linker histone H1 to chromatin and induces an extended chromatin fiber conformation, *J. Biol. Chem. 280*, 34063−34072.
37. Zlatanova, J., Leuba, S. H., and van Holde, K. (1998) Chromatin fiber structure: Morphology, molecular determinants, structural transitions, *Biophys. J. 74*, 2554−2566.
38. Cotton, R. W., and Hamkalo, B. A. (1981) Nucleosome dissociation at physiological ionic strengths, *Nucleic Acids Res. 9*, 445−457.
39. Garcia de la Torre, J., Navarro, S., López Martínez, M. C., Díaz, F. G., and López Cascales, J. J. (1994) HYDRO: A computer software for the prediction of hydrodynamic properties of macromolecules, *Biophys. J. 67*, 530−531.
40. Butler, P. J., and Thomas, J. O. (1998) Dinucleosomes show compaction by ionic strength, consistent with bending of linker DNA, *J. Mol. Biol. 281*, 401−407.
41. Mann, R. K., and Grunstein, M. (1992) Histone H3 N-terminal mutations allow hyperactivation of the yeast GAL1 gene in vivo, *EMBO J. 11*, 3297−3306.
42. Wan, J. S., Mann, R. K., and Grunstein, M. (1995) Yeast histone H3 and H4 N termini function through different GAL1 regulatory elements to repress and activate transcription, *Proc. Natl. Acad. Sci. U.S.A. 92*, 5664−5668.
43. Deckert, J., and Struhl, K. (2001) Histone acetylation at promoters is differentially affected by specific activators and repressors, *Mol. Cell. Biol. 21*, 2726−2735.
44. Shogren-Knaak, M., Ishii, H., Sun, J. M., Pazin, M. J., Davie, J. R., and Peterson, C. L. (2006) Histone H4-K16 acetylation controls chromatin structure and protein interactions, *Science 311*, 844−847.
45. Bash, R. C., Yodh, J., Lyubchenko, Y., Woodbury, N., and Lohr, D. (2001) Population analysis of subsaturated 172-12 nucleosomal arrays by atomic force microscopy detects nonrandom behavior that is favored by histone acetylation and short repeat length, *J. Biol. Chem. 276*, 48362−48370.
46. Garcia-Ramirez, M., Rocchini, C., and Ausio, J. (1995) Modulation of chromatin folding by histone acetylation, *J. Biol. Chem. 270*, 17923−17928.
47. Hamiche, A., Carot, V., Alilat, M., De Lucia, F., O'Donohue, M. F., Révet, B., and Prunell, A. (1996) Interaction of the histone (H3−H4)2 tetramer of the nucleosome with positively supercoiled DNA minicircles: Potential flipping of the protein from a left- to a right-handed superhelical form, *Proc. Natl. Acad. Sci. U.S.A. 93*, 7588−7593.
48. Leuba, S. H., Bustamante, C., van Holde, K., and Zlatanova, J. (1998) Linker histone tails and N-tails of histone H3 are redundant: Scanning force microscopy studies of reconstituted fibers, *Biophys. J. 74*, 2830−2839.
49. Leuba, S. H., Bustamante, C., Zlatanova, J., and van Holde, K. (1998) Contributions of linker histones and histone H3 to chromatin structure: Scanning force microscopy studies on trypsinized fibers, *Biophys. J. 74*, 2823−2829.
50. Sato, M. H., Ura, K., Hohmura, K. I., Tokumasu, F., Yoshimura, S. H., Hanaoka, F., and Takeyasu, K. (1999) Atomic force microscopy sees nucleosome positioning and histone H1-induced compaction in reconstituted chromatin, *FEBS Lett. 452*, 267−271.
51. d'Erme, M., Yang, G. L., Sheagly, E., Palitti, F., and Bustamante, C. (2001) Effect of poly(ADP-ribosyl)ation and Mg^{2+} ions on chromatin structure revealed by scanning force microscopy, *Biochemistry 40*, 10947−10955.
52. Graziano, V., Gerchman, S. E., Schneider, D. K., and Ramakrishnan, V. (1996) Neutron scattering studies on chromatin higher-order structure, *Basic Life Sci. 64*, 127−136.

BI060807P